Coarse-graining procedure to generate and analyze heterogeneous materials: Theory

Raphael Blumenfeld and Salvatore Torquato
Princeton Materials Institute, Princeton University, Bowen Hall, 70 Prospect Avenue, Princeton, New Jersey 08540-5211
(Received 8 April 1993; revised manuscript received 30 June 1993)

We present a theoretical framework to generate and statistically characterize the microstructure of coarse-grained random two-phase heterogeneous materials. The structures are produced by convolving the intensity function $f(\mathbf{x})$ of a source image with a kernel $K(\mathbf{x})$ to yield a new smoothed intensity $F(\mathbf{x})$ and then using the coarse-grained image which results from taking a cut through the surface $F(\mathbf{x})$ at F_0 ("islands within lakes"). By varying F_0 and the properties of the kernel K, one can generate a wide class of intricate microstructures. We provide a general means, which heretofore had been lacking, of representing and computing the correlation functions that statistically characterize samples of arbitrary size of such coarse-grained models. To illustrate our formalism we obtain results for specific examples of the source intensity $f(\mathbf{x})$ and the kernel K. We also show how one can use this procedure to generate media consisting of distinct particles in a matrix of another material. The applicability of this study to bulk properties of heterogeneous materials and to image analysis in general is discussed.

PACS number(s): 81.35.+k, 05.40.+j, 42.30.−d

I. INTRODUCTION

Heterogeneous materials abound in nature and in man-made situations. Examples include ceramic composites, geologic media, polymer blends, foams, colloidal dispersions, and animal and plant tissue, to mention but a few. The microstructures of these materials are typically quite complex in that they are characterized by some degree of randomness and possess intricate topologies. The macroscopic properties of random heterogeneous materials are generally sensitive to the details of the microstructure [1–5]. Thus an important fundamental aspect of theoretically understanding the macroscopic behavior of such media is to be able to generate and characterize suitable model microstructures.

Over the last decade considerable effort has been expended in characterizing the microstructure of media composed of random distributions of finite-sized particles [5]. By allowing the particles to overlap in varying degrees and possess arbitrary shape and size, particle-based models can be made to be quite versatile. For example, such particle-based models can represent both unconsolidated media (e.g., beds of particles) and consolidated media (e.g., sintered materials).

Following the work of Weinrib and Halperin [6], Crossley, Schwartz, and Banavar [7] proposed recently a class of models of porous media based on the smoothing of random white-noise images using either Gaussian or Laplacian-Gaussian kernels. The models consist of convolving a source intensity function $f(\mathbf{x})$ with a kernel $K(\mathbf{x})$ to yield a new function $F(\mathbf{x})$, where the coarse-grained image is a cut through the surface $F(x)$ at F_0. This generates a two-phase composite medium. Using computer simulations, they showed that with the proper choice of smoothing parameters, models of this type give a reasonable image representation of Vycor glass and crystalline dolomites. Image analysis techniques are currently being used to study properties of cementatious materials [8].

The morphology of the coarse-grained image depends on the intensity $f(\mathbf{x})$, the kernel K, and the cutoff value F_0. By varying these quantities, coarse-grained models can be made to represent the microstructure of a wide class of heterogeneous materials. Despite the wide range of applicability of this technique, there is presently no systematic theoretical analysis of the statistical characteristics of the corresponding microstructures and their bulk properties.

The purpose of the present paper is to provide a theoretical framework to generate and statistically characterize the microstructure of such models and their generalizations. In particular, we provide a general formalism to represent and compute correlation functions that statistically characterize the microstructure of finite-sized samples of the models. We apply the formalism to a number of different source intensities and kernels. One of our aims here is ultimately to be able to study the effect of varying the above quantities on the morphology and the macroscopic behavior of the material. Some of the expressions obtained here for the correlation functions arise in rigorous relations for the effective conductivity [1,3,5] and elastic moduli [2,5] of composite materials, rate constant of diffusion between traps [5], and the fluid permeability of porous media [5]. Thus knowledge of such information will enable one to compute all these quantities for this rich class of morphologies. We also show that models of particle-based materials may be viewed as special cases of coarse-grained models for certain f, K, and F_0.

The outline of this paper is as follows. In Sec. II we formulate the basic problem. In Sec. III we analyze the statistical properties of the smoothed image. We illustrate our results by explicitly analyzing two particular examples: Gaussian and binary intensities of the source image. In Sec. IV we analyze the statistical correlation functions associated with the coarse-grained image that result after cutting the surface $F(\mathbf{x})$ at F_0. We show that particulate systems that are generated by particular

1063-651X/93/48(6)/4492(9)/$06.00

choices of the parameters of the coarse-graining procedure can be made to reproduce almost exactly a Poisson distribution of overlapping monodisperse particles within a matrix. Some of our results for Gaussian kernels are demonstrated in arbitrary dimensions. Finally, we summarize our results and briefly discuss them in Sec. V.

II. PROBLEM FORMULATION

We start from an original system of N points, distributed in some fashion throughout a d-dimensional volume. This system we term the source, and we will refer to the points as source points. Let $\mathbf{x}_n$ $(n=1,2,\ldots,N)$ be the position vector of the nth point. With each point we associate a scalar f_n that represents some measurable quantity of interest, which we henceforth call the intensity. For example, the points can represent a set of stellar objects that one would like to observe and analyze, and f_n would be the intensity of radiation emitted by the nth star. As another example, the points can represent the centers of areas in the source system, with electrical conductivity of magnitude f_n. In principle, the points can either fill the source uniformly or they can be randomly distributed within the volume of the source. Thus we have a spatial distribution of such source points, for which we now define a global measure (intensity) $f(\mathbf{x})$ at position $\mathbf{x}$ as

$$f(\mathbf{x})=\sum_{n=1}^{N} f_n \delta(\mathbf{x}-\mathbf{x}_n) , \tag{2.1}$$

where $\delta(\mathbf{x}-\mathbf{x}_n)$ indicates a d-dimensional δ function. Let us term $f(\mathbf{x})$ the source function.

Having defined the source and the source function, we wish now to specify a procedure that maps the source onto an image that is a coarse-grained replica of the source. A general way to define such a procedure would be

$$F(\mathbf{x},\{C\})=\int f(\mathbf{x}')K(\mathbf{x}-\mathbf{x}',\{C\})d^d\mathbf{x}' . \tag{2.2}$$

In the language of image science, $F(\mathbf{x})$ is the distribution of the intensity of the smoothed image. The kernel K is also called the filtering function, the filter, and the point spreading function, in the language of image synthesis. For simplicity, we assume that $K(\mathbf{x},\{C\})$ is a scalar function that is even when $\mathbf{x}\rightarrow-\mathbf{x}$. Therefore, one of the effects of this kernel is to smear the pointlike intensities of the point sources. The kernel can also be made to rescale the size of the system, as well as translate it, by $K(\mathbf{x})=K[A+\mathbf{x}/\omega]$. Generally, the kernel can depend on a set of M parameters $\{C\}$, of which A and ω are only two elements. Furthermore, in principle, this set can either consist of predetermined elements, or these parameters can be randomly chosen from a respective set of given distributions.

Now there are several questions that one can address.

(i) Suppose K is predetermined, which includes knowledge of its functional form as well as knowledge of the exact values of the elements of $\{C\}$. What is the interdependence between the statistics of the distribution of the intensities of the source f and the statistics of the intensity of the image F? This issue can be important when measurements are inaccessible on the source (image) and accessible on the image (source). For example, suppose the source points represent regions of high conductivity (high intensity) within a poorly conducting matrix (dark background). We can then interpret F as the spatial distribution of the conductivity within the image and measure the effective bulk conductivity of the image. This effective conductivity has a distribution, and the question is how can this distribution be made to tell us about the distribution of the effective conductivity of the source?

(ii) Suppose the process by which the source was created is unknown. Can we infer on the statistics of this process from the statistics of F? An example where such a question is relevant would be in astrophysics, where the stochastic process, by which stellar objects (galaxies, stars, etc.) were formed, is of much interest. In this case we view the system of bright objects through some apparatus, which already creates an image of the source data. This image can be transformed to give birth to a more coarse-grained offspring, and so on and so forth. The goal then is to learn about the stochastic dynamical process that created these objects from the statistics of the images.

(iii) The traditional image synthesis problem: Assume that one is interested in a particular source configuration, namely, a source generated by a specific configuration of the intensities. Also suppose that noise affects the image through the fluctuations of the elements of the set $\{C\}$. The question is, to what accuracy can one retrieve the particular source configuration after it has been distorted by the noise?

(iv) The variability of the elements of $\{C\}$ need not be interpreted as interfering with measurements. There are many situations where the problem is to find the best kernel for a given purpose. In such cases we can determine the functional form of the kernel by tuning its parameters. We can use this variability to optimize the values of these parameters subject to constraints that we can impose. The way to carry out this optimization is to analyze the relationship between the statistics of the source and the statistics of the image, carrying along the undetermined parameters (the elements of C), and then optimize them by constraining either the image or the source.

These issues span too broad a scope to cover in one paper and we cannot address them all here. Rather, we concentrate on the first problem. Some of the other directions are currently under investigation, and further results will be reported in forthcoming papers. Nevertheless, the formulation and the analysis presented here are also intended to lay the foundations and pave the way for further study regarding these other aspects of coarse-graining.

III. ANALYSIS: THE SMOOTHED IMAGE

In the following we grid-discretize the source, by associating each source point with a d-dimensional vector, whose components are integral multiples of the grid unit separation a (the mesh size). Thus the index n becomes a vectorial quantity $\mathbf{n}$, and the positions of the source

points are $\mathbf{x}_n=(n_1,n_2,\ldots,n_d)a$. We choose to treat discretized images (i.e., n_j runs over all integer values up to the size of the system) because, in practice, one works with a digital-based image. Our analysis requires only simple modifications to apply to continuum images as well. Note that by assuming that the source points homogeneously fill the volume of the source system we have not lost the generality of a random distribution. We can always assign a finite probability for f_n to be zero and associate the occurrence of $f_n=0$ with nonexistence of the nth source point or with the background intensity. So by introducing randomness *only* in f_n we have obviated the need to specify the distribution of the locations of the source points.

In the most general case the intensities can be chosen from N different probability densities (PD)'s, $p_n(f_n)$. These PD's can be either correlated or uncorrelated. We choose to focus here on the case where there is no correlation between the p_n's. Namely, $p_n df_n$ is the probability of finding the intensity of the nth point between a value of f_n and a value of f_n+df_n. Before continuing, let us define the characteristic function (CF) of the nth PD,

$$\phi_n(k_n)=\int_{-\infty}^{\infty} e^{ik_n f_n} p_n(f_n)df_n \ . \tag{3.1}$$

The value of $F(\mathbf{x})$ can be written in the form

$$F(\mathbf{x})=\sum_{n=1}^{N} f_n K(\mathbf{x}-\mathbf{x}_n) \ . \tag{3.2}$$

For brevity, we drop the explicit dependence on $\{C\}$, and for the purpose of the present study, we assume that its elements are completely specified.

Since Eq. (3.2) is written in a convolution form, the Fourier transform of F is simply

$$\mathcal{F}(\omega)=f(\omega)\mathcal{K}(\omega) \ , \tag{3.3}$$

which is the main tool used presently in the field of image analysis. However, for our purpose here, whether we study F or $\mathcal{F}$ does not change the level of difficulty, and we find it more convenient to discuss F. It is simple to show that if the PD of F is $P(F)$ then the CF of $P(F)$ is

$$\Phi_F(k)=\prod_{n=1}^{N} \phi_n[kK_n] \ , \tag{3.4}$$

where $K_n\equiv K(\mathbf{x}-\mathbf{x}_n)$. We are now in a position to study some of the statistical properties of F. In the following we will denote by $\langle A(\mathbf{x})\rangle=\int A(\mathbf{x})[\prod_{n=1}^{N} p_n(f_n)df_n]$ an ensemble average over the distribution of intensities and by $\overline{A}=(1/V)\int A(\mathbf{x})d^d\mathbf{x}$ a volume average over $\mathbf{x}$. These two averages of F are

$$\langle F\rangle=\sum_n \langle f_n\rangle K_n$$

and

$$\overline{F}=\sum_n f_n \int \frac{d^d\mathbf{x}}{V} K_n \ ,$$

where V is the volume of the source. Note that carrying both averages out on F results in a sum of decoupled averages over the intensities and the volume. This statement is also true for any power of F, as well as for its higher-order correlations. Let us consider the intensity-intensity correlation function of the image $C_2(\mathbf{y})=F(\mathbf{x})F(\mathbf{x}+\mathbf{y})$. Its expectation value over all realizations of the intensity function can be calculated in terms of correlations between intensities, f_n, and spatial correlations, $D_{n,m}$ in the source

$$\langle \overline{C_2(\mathbf{y})}\rangle=\sum_{n,m}\langle f_n f_m\rangle D_{n,m}(\mathbf{y}) \ , \tag{3.5}$$

where

$$D_{n,m}(\mathbf{y})\equiv\int d^d\mathbf{x} K(\mathbf{x}-\mathbf{x}_n)K(\mathbf{x}+\mathbf{y}-\mathbf{x}_m) \ .$$

Note that when the intensities are uncorrelated, the intensity-intensity correlation function in the source decomposes into a product of the averages, $\langle f_n\rangle\langle f_m\rangle$, while the diagonal terms $n=m$ give the second moments of f_n, $\langle f_n^2\rangle$. If, in addition, all the intensities are chosen from an identical distribution, namely, $p_n=p\,;\forall n$, the expectation value of intensity-intensity correlation function simplifies to

$$\langle \overline{C_2(\mathbf{y})}\rangle=\langle f_n\rangle^2\sum_{n\neq m} D_{n,m}(\mathbf{y})+\langle f_n^2\rangle\sum_n D_{n,n}(\mathbf{y}) \ . \tag{3.6}$$

It is easy to see that higher-order correlations decompose similarly into a product of spatial correlations involving only the kernel function at different locations and correlations among intensities of different source points. In what follows, we carry out explicit analyses for two particular examples.

A. Gaussian intensities

Consider first the case when the intensities are chosen randomly from N Gaussian distributions. Namely,

$$p_n(f_n)=A(\gamma_n,\sigma_n)\exp[-(f_n-\gamma_n)^2/(2\sigma_n^2)] \ , \quad \{0\le f_n\le 1\} \ , \tag{3.7}$$

where the normalization constant A is

$$A(\gamma_n,\sigma_n)=\frac{\sqrt{2/\pi}}{\sigma_n[\Phi((1-\gamma_n)/(\sqrt{2}\sigma_n))+\Phi(\gamma_n/(\sqrt{2}\sigma_n))]} \ ,$$

and $\Phi(x)\equiv\int_0^x \exp(-x^2)dx$. The CF of this distribution is

$$\phi_n(k_n)=(A(\gamma_n,\sigma_n)/A(\epsilon_n,\sigma_n))\times\exp[-\sigma_n^2(k_n-i\gamma_n/\sigma_n^2)^2-\gamma_n^2/2\sigma_n^2] \ , \tag{3.8}$$

where $\epsilon_n\equiv\gamma_n+i\sigma_n^2 k_n$. We want to find the probability density $P(F)$ by using (3.4). For simplicity we assume that $\sigma_n\ll\min\{1,\gamma_n\}$, although this assumption is not essential in any way to the derivations in this work. The simplification is that $\Phi\simeq 1$ in the above expressions. The characteristic function of P is

$$\Phi_F(k)=\exp[-\Gamma^2/(2\Sigma^2)-(\Sigma^2/2)(k-i\Gamma/\Sigma^2)^2] \ , \tag{3.9}$$

where

$$\Gamma \equiv \sum_n \gamma_n K_n, \quad \Sigma^2 \equiv \sum_n \sigma_n^2 K_n^2 . \tag{3.10}$$

It is simple to carry out the inverse transform to find the PD of F. Specifically, we get

$$P(F)=(\sqrt{2\pi}\Sigma)^{-1}\exp[-(F-\Gamma)^2/(2\Sigma^2)] , \tag{3.11}$$

identifying Γ and Σ as the mean and the width of the distribution of F. Note that this result is general for any choice of kernel K. For example, let us consider Gaussian kernels, which are very widely used in the literature of image analysis,

$$(K(\mathbf{x})=\exp[-|\mathbf{x}|^2/\omega^2] ,$$

where ω is a scaling factor. In this case the series in (3.10) can be summed, and the mean of F and its variance over the intensities can be found analytically. In one dimension this calculation gives for these parameters

$$\begin{aligned}\Gamma &= (\omega/a)\theta_3(-x\pi/a, \exp[-(\pi\omega/a)^2])\gamma , \\ \Sigma^2 &= (\omega/\sqrt{2}a)\theta_3(-x\pi/a, \exp[-(\pi\omega/\sqrt{2}a)^2])\sigma^2 .\end{aligned} \tag{3.12}$$

For the sake of convenience, we have assumed in these expressions that all the intensities are chosen from the same distribution, characterized by γ and σ. The function θ_3 is the elliptic theta function [9], and a is the mesh size that enters through $\mathbf{x}=\mathbf{n}a$. In a higher dimension d, each point is characterized by d indices, $n_1, n_2, \ldots, n_d$. The kernel can then be written as

$$K(\mathbf{x})=\prod_{m=1}^{d}\exp[-(x^{(m)}-x_n^{(m)})^2/\omega^2] , \tag{3.13}$$

where $x^{(m)}$ and $x_n^{(m)}$ are the components of $\mathbf{x}$ and $\mathbf{x}_n$ in the m direction. To find now the average Γ and the width Σ of the PD of F, we need to sum then over all d indices, which is straightforward in the Gaussian case and leads to

$$\begin{aligned}\Gamma_d &= \prod_{m=1}^{d}\sum_{n=1}^{N}\exp[-(x^{(m)}-x_n^{(m)})^2/\omega^2] \\ &= \left[\frac{\omega\gamma}{a}\right]^d \prod_{m=1}^{d}\theta_3(-x^{(m)}\pi/a, \exp[-(\pi\omega/a)^2]) , \\ \Sigma_d^2 &= (\omega\sigma^2/\sqrt{2}a)\prod_{m=1}^{d}\theta_3(-x^{(m)}\pi/a, \exp[-(\pi\omega/\sqrt{2}a)^2]) .\end{aligned} \tag{3.14}$$

B. Binary intensities

As another example consider a source consisting of a random set of white and black pixels. Such a color distribution can be described in our language with the set of intensities chosen from the following PD:

$$p_n(f_n)=[\delta(f_n-1)+\delta(f_n+1)]/2 , \tag{3.15}$$

with the understanding that $f_n=1$ (-1) corresponds to a white (black) pixel. This corresponds to having, on average, a 50%-50% mixture of white and black pixels. We are again assuming no spatial correlations between choices of colors at different positions. The CF of p_n is $\phi_n(k_n)=\cos(k_n)$, which gives for the CF of $P(F)$

$$\Phi(k)=\prod\cos[kK_n] . \tag{3.16}$$

This CF can be rewritten in the form

$$\Phi(k)=2^{-N}\sum_{\{s_n\}}\exp\left[ik\sum_{n=1}^{N}s_nK_n\right] , \tag{3.17}$$

where the summation in the exponential is carried out over all possible permutations of $s_n=\pm 1$. It is interesting to note that this form resembles very much a statistical-mechanical trace over the partition function of a system of classical Ising spins (i.e., spins that can attain only two states, $s_n=\pm 1$) in a position-dependent external magnetic field whose magnitude is K_n [10]. The inverse transform is easy to carry out, and it yields

$$P(F)=2^{-N}\sum_{\{s_n\}}\delta\left[F-\sum_{n=1}^{N}s_nK_n\right] , \tag{3.18}$$

where the first summation is again over all possible permutations of $\{s_n\}$. This PD can be immediately checked to be normalized; since each s_n can have two values that are independent of the rest, there are 2^N possibilities of different s_n configurations. An integration over F will give one for each term in the sum, as long as the argument of the δ function vanishes within the range of integration. It follows that the total value integrates to unity. It is not difficult to generalize this distribution to the case where the intensities can assume a discrete number of color values between black and white, namely, when shades of grey can also occur. From Eq. (3.18) we immediately note that the expectation value of F for this distribution is zero. This is so because in the summation over s_n for each configuration $\{s_n\}$ there is an equivalent configuration with each $s_n \rightarrow -s_n$ that occurs with exactly the same probability. Thus $P(F)$ is symmetrical and its mean vanishes. This value corresponds to an in-between grey, which is exactly what we would expect intuitively from a 50%-50% random distribution of black and white regions to display. This example can also be generalized to the case where the black and white pixels do not occur with the same probability. Namely, when Eq. (3.15) is written in the form

$$p_n(f_n)=p\delta(f_n-1)+(1-p)\delta(f_n+1) . \tag{3.19}$$

The second moment of the PD [Eq. (3.18)] is also simple to calculate

$$\Sigma^2=2^{-N}\sum_{\{s_n\}}\left[\sum_{n=1}^{N}s_nK_n\right]^2 . \tag{3.20}$$

Note that the above quantities depend on the spatial coordinates $\mathbf{x}$ through the kernels K_n. A volume integration operates then only on the kernels, and global volume averages are therefore easy to analyze in terms of the individual volume averages of K_n. This simplification holds for the spatial correlations of F as well, in the sense that these correlations can be expressed in terms of sim-

ple sums over correlations between individual K_n functions similar to $D_{n,m}(\mathbf{y})$ above.

IV. ANALYSIS: PLANAR CUTS THROUGH $F(\mathbf{x})$

A. Formulation

We now turn to study the morphological structure of a cut through the surface F at a level F_0. Such a cut defines $(d-1)$-dimensional contours where F intersects the cutting hyperplane. These contours divide the hyperplane into regions that are considered within the contours and complementary external regions. This is the well-known "islands within lakes" picture [11]. For example, in $d=1$, $F(\mathbf{x})=F(x)$, which can be cut by a straight line at F_0. The intersections of $F(x)$ with this line form a set of one-dimensional "chords" that lie in the shade of F, namely, where $F(x)>F_0$. An example is shown in Fig. 1(a). In $d=2$, $F(\mathbf{x})$ defines a two-dimensional surface, which we can cut by a two-dimensional plane at height F_0. The intersection of this plane with F defines now a set of one-dimensional contours enclosing two-dimensional areas where $F(\mathbf{x})>F_0$. Such a cut is illustrated in Fig. 1(b). For simplicity, and to demonstrate our results in the clearest way, we choose to focus here on the one-dimensional case, which allows for simple exact analysis. In future work we will report results in higher dimensions.

B. Correlation functions

In the one-dimensional case, a cut at F_0 yields a set of intersection points ζ_i, which we order in an increasing value. Namely, $i=1$ corresponds to the leftmost intersection that is also of lowest value of x, and so on to the rightmost point, ζ_s. Since we expect $F(x)$ to decay as the boundary of the system is approached, we can safely assume that $F(x)$ increases with increasing x at ζ_1. Thus the intersections with odd and even indices define left and right boundaries of a chord, respectively. We are interested here in the correlation functions associated with the *chord* phase.

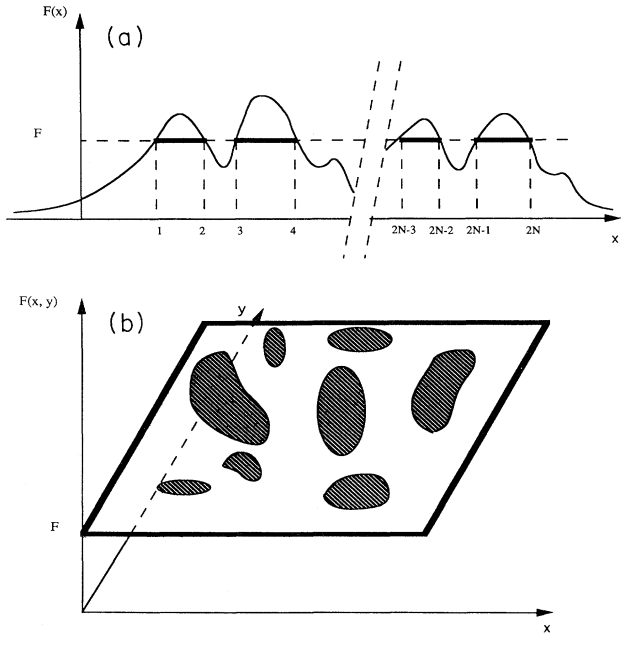

FIG. 1. Examples of a binary phase mixture formed by cuts of $F(\mathbf{x})$: (a) Set of points $\zeta_n(n=1,2,\ldots,2N)$ defined by cutting $F(x)$ with a line at F_0; (b) Set of line contours defined by cutting $F(x,y)$ with a two-dimensional plane at F_0.

We first calculate the expectation value of the volume fraction of these chords q. For a given configuration of the source (whose volume here is assumed to be $2L$)

$$S_1=\frac{1}{2L}\int_{-L}^{L}\Theta(F-F_0)dx\ , \tag{4.1}$$

where $\Theta(x)$ is the step function defined to be 1 for $x>0$ and zero for $x<0$. Therefore the expectation value for the volume fraction of chords is

$$\langle S_1\rangle=\int P(F)S_1dF=\int_{F_0}^{\infty}P(F)dF\ . \tag{4.2}$$

Not surprisingly, this is exactly the probability of finding values of F that are larger than F_0. It is clear that this result is not restricted to $d=1$ and is applicable to any dimensionality. The cumulative distribution of $P(F)$ should be very easy to calculate from the analysis given in the previous section, and therefore the volume fraction of the shaded areas is straightforward to obtain for a given system.

Next we note that *all* higher-order correlations within the chord phase can be written in the form

$$S_n(y_1,y_2,\ldots,y_{n-1})=\frac{1}{2L}\int\Theta(F(x)-F_0)\prod_{j=1}^{n-1}\Theta(F(x+y_j)-F_0)dx\ . \tag{4.3}$$

Observe that $\Theta(F(x)-F_0)$ can be written in terms of the auxiliary function $I(x)$ as follows:

$$\Theta(F(x)-F_0)=I(x)=\sum_{i=1}^{s}\Theta(R_i-|x-r_i|)\ , \tag{4.4}$$

where

$$R_i=\frac{(\zeta_{2i}-\zeta_{2i-1})}{2},\quad r_i=\frac{(\zeta_{2i}+\zeta_{2i-1})}{2}\ ,$$

and $2s$ is the total number of intersection points [12]. Here $2R_i$ and r_i are the length and the centroid position of the ith chord, respectively. By rewriting the correlation function (4.3) as

$$S_n(y_1,\ldots,y_{n-1})=\frac{1}{2L}\int I(x)\prod_{j=1}^{n-1}I(x+y_j)dx\ , \tag{4.5}$$

this formulation permits a simplification as follows: Noting that the set $\{\zeta_i\}$ is nothing but the zeros of the function $F-F_0$, we immediately see that the zeros of $F(x+y_j)-F_0$ are $\{\eta_i=\zeta_i-y_j\}$. Substituting this into Eq. (4.3) facilitates the calculation of the integral. The only computational difficulty lies now in the need to calculate the roots of $F(x)-F_0$. Once this is done one can compute the R_i and r_i, construct the product of the func-

tions I in the integral, and calculate very easily the correlation functions to any order. Since there are many simple algorithms to find the zeros of a one-dimensional function, this method simplifies significantly the calculation of these correlation functions. Moreover, it is possible to find a *polynomial,* whose roots coincide with the roots of the function F, as shown in the Appendix, and use it to find the set $\{\zeta_i\}$.

We illustrate this method by considering the details of obtaining the two-point correlation function within the chord phase. For a particular configuration of source points, the two-point function according to Eq. (4.4) and (4.5) is given by

$$S_2(y)=\frac{1}{2L}\sum_{i,j=1}^{s}\int\Theta(R_i-|x-r_i|)\times\Theta(R_j-|x+y-r_j|)dx\ .$$

The above integrand consists of regions of zeros and ones. Figure 2 shows a particular example of $I(x)$ and $I(x-y)$ along with the overlapping regions that are the only regions that contribute to the integral. A simple inspection of Fig. 2 will convince the reader that this volume is invariant under $y\rightarrow -y$, indicating that $S_2(y)$ is an even function of y. We therefore consider only $y\geq 0$. With the help of Fig. 2 it is not difficult to see that summing over these regions yields

$$S_2(y)=\frac{1}{2L}\sum_{i=1}^{s}v_{2,ii}^{\rm int}(y)+\frac{1}{2L}\sum_{\substack{i,j=1\\(i\neq j)}}v_{2,ij}^{\rm int}(y)\ , \tag{4.6}$$

where the intersection volume

$$v_{2,ij}^{\rm int}(y)=\begin{cases}0, & |y-r_{ij}|>R_j+R_i\\ 2R_i, & |y-r_{ij}|<R_j-R_i\\ R_j+R_i-|y-r_{ij}|, & R_j-R_i\leq|y-r_{ij}|\leq R_j+R_i\ ,\end{cases}$$

where $r_{ij}\equiv|r_j-r_i|$, and we have assumed, without loss of generality, that $R_j>R_i$. This result can now be easily generalized to higher-order correlation functions S_n. The summation in that case would involve n indices, and the terms would have a form similar to (4.6), but with all possible permutations of the roots and the distances y_i's. To find the expectation value of $S_2(y)$ over all possible realizations with 2_s zeros, all we now need to do is weigh the above expression by the probabilities of occurrences of the various roots and integrate over the densities. This process is somewhat involved because for each realization of F [with PD $P(F)$ in functional space F] we have a distinct set $\{\zeta\}$, but notice that the first term is independent of the centroidal positions r_i.

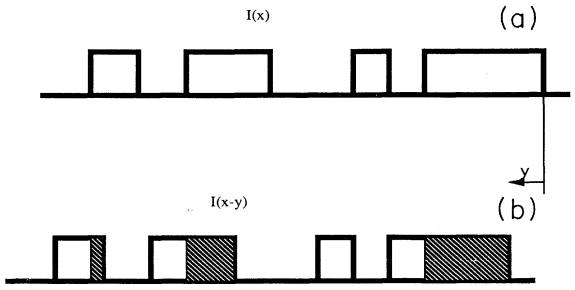

FIG. 2. Contribution to the two-point correlation function in the chord phase in one dimension: (a) Auxiliary function $I(x)$ defined by Eq. (4.4) is unity in the chord phase and zero otherwise. (b) Shifted auxiliary function $I(x-y)$. The overlap region that contributes to S_2 is shaded.

C. Illustrative example: Binary intensity and distribution of particles

To discuss a specific example for the correlation function S_2 let us consider a source where the PD of f_n is given for all f_n by

$$p(f_n)=(1-p)\delta(f_n)+p\delta(f_n-1)\ . \tag{4.7}$$

This PD indicates that each site has a probability p (or $1-p$) to have intensity $f_n=1$ (or 0). In a given realization, and for a large number of points, we expect, on the average, a fraction p of the source points to emit at intensity $f_n=1$, while the rest of the points with zero intensity are considered as the background. The probability of finding exactly s points at positions $x_1,x_2,\ldots,x_s$ in a single realization is $p^2(1-p)^{N-s}$. The image F is

$$F(x)=\sum_{n\in\Gamma(p)}K(x-x_n)\ , \tag{4.8}$$

where $\Gamma(p)$ is the set of all points in the source for which $f_n=1$. We assume that $K(x)$ is a function that is symmetric about $x=0$, where it also takes on its maximum, and that it decays monotonically away from $x=0$. The assumption that K is even in its argument is made for simplicity and by no means poses a restriction; the following example can be easily discussed in the absence of this simplification. Since the source points are randomly distributed within the source volume V, the typical distance between two neighboring source points in a realization with s points is $\lambda=[V/s]^{1/d}$.

We now discuss two case studies: one of a low concentration of source points and the other of high concentration. Let $F_0=K(0)(1-\delta)$, where $\delta\ll 1$. In this case only the very top of each smeared point is cut and the initial source points transform into small regions (rods in $d=1$, circles in $d=2$, etc.). The locations of these regions are centered predominantly around the locations of the initial source points, which were randomly distributed. As we lower the level F_0 at which the image is cut, the regions grow until they start to overlap. By lowering the F_0 plane we then simply increase the radii of the randomly placed circles ($d=2$) or rods ($d=1$) and let them overlap eventually. When the density of the system is such that interference between $K(x-x_n)$ and $K(x-x_m)$ for $n\neq m$ is negligible, we can solve approximately for the locations of the zeros for a given value of F_0 by finding the value of the radii of the rods from the equation

$$K(R)=F_0\ . \tag{4.9}$$

In $d=1$ this yields two roots for a monotonically decreasing kernel. If there is no overlap between rods it is simple to express the location of zeros in terms of the locations of the source points

$$\zeta_{2i-1}=x_i-R,\quad \zeta_{2i}=x_i+R\ ,$$

where the indexing of the positions i increases with the value of x_i from left to right. Thus, using the definitions immediately below (4.4), we have

$$R_i=R,\quad r_i=x_i\ .$$

Having found the zeros, we can now substitute them in expressions (4.5) or (4.4) to find the correlation functions in terms of the location of the initial source points.

It is clear that the simplification in this dilute regime is effected by the correspondence to values of F_0 that are close to $K(0)$. In this case the volume fraction of a particular s-point realization is $S_1=2Rs/2L$. An ensemble average over all possible values of s would yield $\langle S_1\rangle\approx p$, as expected. In the dilute regime $\langle S_1\rangle$ is very close to p.

The two-point correlation function within the rod phase can be found from (4.6) exactly to order $s/2L$ as

$$S_2(y)=\frac{s}{2L}v_{2,ii}^{\rm int}(y)\ . \tag{4.10}$$

Note that here $v_{2,ii}^{\rm int}(y)$ has a very simple interpretation: it is the intersection volume of two rods of length $2R$ whose centroids are separated by a distance y. In the limit $s\to\infty$, $L\to\infty$ such that $s/2L$ remains constant, (4.10) recovers the well established result for a dilute distribution of monodisperse rods [5,13]. To carry out an ensemble average of $S_2(y)$ we need to weigh this expression by the probability of finding this particular configuration $[=p^s(1-p)^{N-s}]$, sum over all possible values of S_2 with s points, and then sum over s. However, if we are just interested in the subset of all configurations with s points, we have to sum only over contributions from this partial ensemble of sources. The total number of such configurations is $\binom{N}{s}p^s(1-p)^{N-s}$, and so the probability of finding a system with s source points among all possible systems is $Q_s=\binom{N}{s}p^s(1-p)^{N-s}2^{-N}$. Since the locations of the source points are independent we can assign for each point x_n a uniform probability of being found in the volume of the source, $1/2L$. It is straightforward to integrate (4.6) over all probabilities of the x_n's and obtain the expectation value $|S_2(y)|_s$ over this partial ensemble. To find the ensemble average over all systems, permitting any number of point sources, all we need to do is multiply $|S_2(y)|_s$ by Q_s and sum over s. This is a simple exercise given that $|S_2(y)|_s$ can be related to the second derivative of a binomial sum with respect to p. We emphasize that the calculation in the nonoverlapping regime is straightforward to generalize to higher dimensions.

Turning to high concentrations of source points we now claim that we can choose F_0 such that the resulting chord distribution that is generated is almost identical to the distribution of monodisperse rods placed randomly on a segment line. We demonstrate this by computing the characteristic function $I(x)$ and the two-point correlation function $S_2(y)$ for both models. Initially $N=500$ points are randomly distributed along a line segment of length $2L$. The distribution is convoluted according to the procedure outlined above with a Gaussian kernel of the form

$$K(x)=\exp[-|x|^2/\omega^2]\ .$$

The width of the kernel $\omega=2L/500$ and $F_0=0.82$ are chosen such that the volume fraction of the chord phase is definitely *not dilute,* i.e., $p\approx 0.634$. We compute $F(x)$ for exactly one realization and plot a representative section of it in Fig. 3. In Fig. 4 we show the corresponding two-point correlation function.

Employing now the same random distribution of 500 source points we place rods of equal size centered on each such point. The size of the rod is chosen to give the same volume fraction of the resulting chord (rod) phase, $p\approx 0.634$. The characteristic function and the two-point correlation function are similarly computed and shown in Figs. 3 and 4. By comparing the computed plots one can immediately observe that the features of the two systems are almost identical. It can be seen by inspecting Fig. 3 that the distributions of the chord phases of the two systems almost coincide. The deviation of the models is only at the very short scale of the size of a rod. These deviations are due to very small dustlike rods that the second method generates, which are not generated by the cut in F. Another demonstration of the close equivalence between the systems can be seen in Fig. 4 where the plots of $S_2(y)$ follow each other closely all the way up to scales of the size of the system. The small deviation of the plots in the short-scale regime can be traced exactly to the above difference. In the long-range scale both plots of $S_2(y)$ exhibit fluctuations that reflect the fact that these are single finite realizations. An ensemble average over such realizations will eliminate these fluctuations.

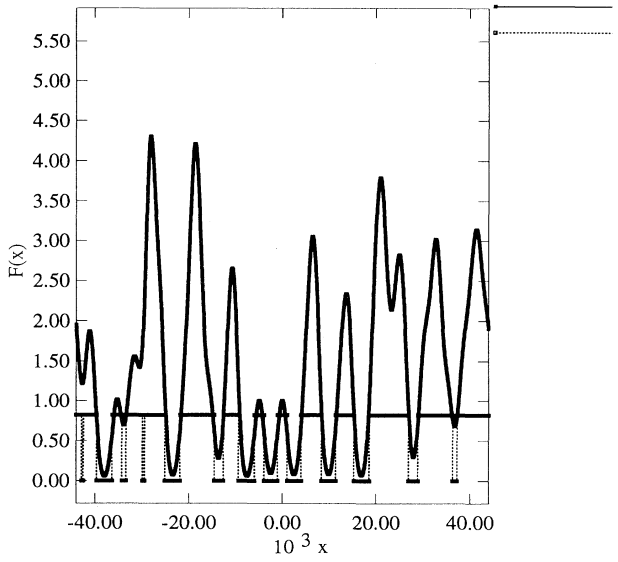

FIG. 3. One-dimensional random system: A cut through F at $F_0=0.82$ and the equivalent characteristic function (normalized to height 0.82 for convenience) of Poisson distributed rods.

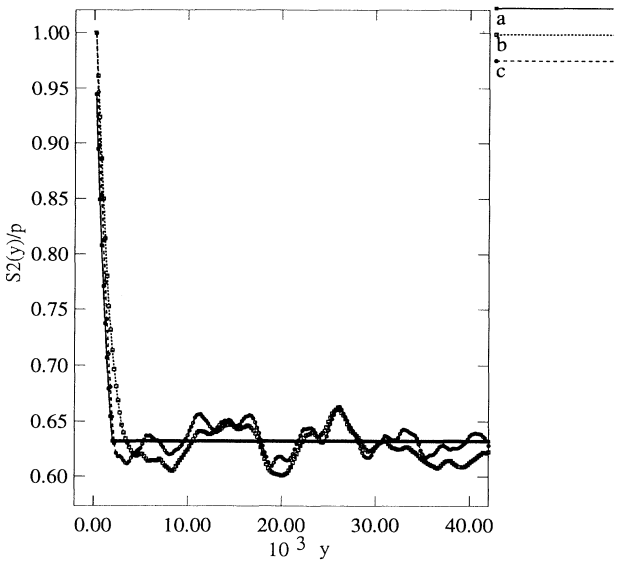

FIG. 4. Two-point correlation function $S_2(y)$ in the chord phase scaled by the chord volume fraction p for (a) the theoretical result for an infinite ensemble, (b) a cut in F, and (c) a Poisson distribution of rods.

Such Poisson distribution of rods on a line is a very well studied problem and therefore enjoys well known theoretical results. In particular the exact form of $S_2(y)$ is known for an infinite ensemble of such rod distributions

$$S_2(y)=\begin{cases} 2p-1+\exp\left[-\dfrac{s(2R+y)}{2L}\right], & y<2R \\ p^2, & y>2R\ , \end{cases}$$

and we have included it in Fig. 4. The theoretical value of $S_2(y)/p$ agrees extremely well with both our computed plots, given the fact that we have used only one system. It is evident that the particular choice of the Gaussian kernel is irrelevant to this result, and any symmetrical kernel that decays on a similar scale as the Gaussian kernel would produce the same equivalence. We have thus shown that the paradigm of the Poisson distribution of monodisperse rods, even in the dense regime, can be generated by our technique for a particular choice of ω and F_0. Note that this result is stronger than simply claiming that the statistics of the models are the same. Rather, by using only one realization we have shown that the *details* of the two generated systems are almost identical.

V. CONCLUDING REMARKS

We have presented a theoretical framework to study a coarse-graining transformation from a source to a smoothed image. We have analyzed the relations between the statistical properties of the source intensity and those of the image. In particular, we have expressed the intensity-intensity correlation functions of the image in terms of the source statistics. For the special case of Gaussian kernels, we have derived explicitly the probability density of the image intensity function F. We have also derived this density for general kernels in the case of a binary source intensity distribution.

Next we have discussed the correlations within the phases that are generated by cuts of the image intensity F. The one-point correlation function, which corresponds to the volume fraction of the chord phase, was shown to relate simply to the cumulative-distribution of F in any dimension. We have analyzed the two-point correlation function and obtained an expression for it in one dimension in terms of the locations of the roots of $F-F_0$. We have outlined in the Appendix two alternative methods to find these roots. Moreover, for a Gaussian kernel and binary intensity distribution, we have calculated the two-point correlation function $S_2(y)$ in one dimension. We have found that this system is almost identical to a Poisson distribution of monodisperse rods.

The results of this study demonstrate that by varying the source intensity $f(\mathbf{x})$, kernel $K(\mathbf{x})$, and cutoff value F_0 coarse-grained models can be made to represent the morphology of practically any heterogeneous material. We have shown that by choosing f, K, and F_0 our coarse-graining procedure can generate distributions of finite-sized particles in a matrix. This is a unique way of producing such particulate morphologies. Weinrib and Halperin [6] studied the value of F_0 at which coarse-grained Gaussian and Laplace-Gaussian transformations percolate, but we have presented here a theoretical formalism that represents and computes correlation functions that statistically characterize the microstructure of such models in general. In particular the n-point correlation functions S_n that we have discussed are required to compute bulk properties such as the effective conductivity [1,3,5], effective elastic moduli [2,5], trapping rate in diffusion [5], and fluid permeability [5]. A significant point that needs to be mentioned is that our analysis is valid for samples of *arbitrary size,* in contrast to traditional studies in heterogeneous materials that typically pertain to infinitely large systems.

In future work we will focus our attention on calculations of the correlation functions of coarse-grained models in two and higher dimensions. We will also separately study the inverse problem mentioned in Sec. II, namely, the inference of the source intensity $f(\mathbf{x})$, and its statistics, given the smoothed intensity of the image $F(\mathbf{x})$, with and without noise in the coarse-graining transformation.

ACKNOWLEDGMENTS

We are indebted to E. Garboczi for bringing this problem to our attention and thank L. Schwartz and B. Liu for useful conversations. We are especially grateful to S. Harris for stimulating discussions and for a critical reading of the manuscript. The support of the Office of Basic Energy Sciences, U.S. Department of Energy, under Grant No. DE-FG02-92ER14275, is gratefully acknowledged.

APPENDIX. ALTERNATIVE WAYS FOR FINDING THE ZEROS OF A FUNCTION

Here we outline two alternative methods to extract the zeros of the function $F(x)-F_0$. The generic functions that are discussed in the text have M zeros, which are predominantly of multiplicity 1, but in some cases may be of multiplicity 2 (this happens exactly when two zeros coalesce). Construct the Cauchy integral

$$G_m=\frac{1}{2\pi i}\oint_C \frac{z^m dF/dz}{F(z)-F_0}dz=\sum_{i=1}^{M} a_i z_i^m \ , \tag{A1}$$

where the contour C is a circle of radius L centered at $x=0$. This formulation works only if $F(z)$ is analytic in, and on, C. The right-hand side of (A1) originates from the residue theorem, and the sum is carried out over all the zeros of the function $F(z)-F_0$ within C; the prefactor a_i is the multiplicity of the ith zero. Carrying out this integral with $m=0$ gives the total number of zeros $G_0=M'\geq M$, where zeros with multiplicity 2 are counted twice. Therefore the first step is to solve for G_0 and to find M'. The next step now depends on taste and computational convenience. One alternative is to progress by constructing the quantities G_m with $m=1,2,\ldots,M'$, obtain a set of M' nonlinear algebraic equations, and then solve for the zeros.

However, suppose that we have a good method for finding zeros of a polynomial, rather than of a general function. In this case we can find the polynomial of order M' whose zeros are exactly $\{\zeta_i\}$. This is done in the following way: Denoting the coefficients of the sought polynomial by c_{m-1} and requiring that the coefficient of $z^{M'}$ is unity, we can use Newton identities to find the values of c_m from the knowledge of G_m. These identities give recursive formulas for the coefficients in the form [14]

$$mc_{s-m}+\sum_{j=1}^{m-1} G_j c_{s-m+j}+G_m=0 \ . \tag{A2}$$

Thus, depending on computational convenience we can either solve the nonlinear equations or we can form a polynomial whose zeros are the same as those of $F(x)-F_0$ and find its zeros by standard numerical routines.

[1] W. F. Brown, J. Chem. Phys. **23**, 1514 (1955).

[2] G. W. Milton and N. Phan-Thien, Proc. R. Soc. London Ser. A **380**, 305 (1982).

[3] M. Beran, *Statistical Continuum Theories* (Wiley, New York, 1968).

[4] J. G. Berryman and S. C. Blair, J. Appl. Phys. **60**, 1930 (1986).

[5] S. Torquato, Appl. Mech. Rev. **44**, 37 (1991). The reader is referred to this review article for a broad range of references.

[6] A. Weinrib and B. I. Halperin, Phys. Rev. B **26**, 1362 (1982).

[7] P. A. Crossley, L. M. Schwartz, and J. R. Banavar, Appl. Phys. Lett. **59**, 3553 (1991).

[8] E. J. Garboczi (private communication).

[9] I. S. Gradshteyn and I. M. Ryzhik, *Tables of Integrals, Series and Products* (Academic, New York, 1965), p. 921.

[10] See, e.g., L. D. Landau and E. M. Lifshitz, *Statistical Mechanics* (Pergamon, Oxford, 1976), p. 198; C. Domb and M. S. Green, *Phase Transitions and Critical Phenomena* (Academic, London, 1972), Vol. 1.

[11] See, e.g., H. Scher and R. Zallen, J. Chem. Phys. **53**, 3759 (1970).

[12] If there are source points that are very close to the boundaries of the system, the number of intersection points, which correspond to the zeros of $F(x)-F_0$, is reduced by one or two, a phenomenon that can also occur in higher dimensions. We disregard this possibility here, noting that it is trivial to take account of such a situation in the treatment presented here.

[13] H. L. Weissberg and S. Prager, Phys. Fluids **5**, 1390 (1962).

[14] See, e.g., W. L. Ferrar, *Higher Algebra,* 2nd ed. (Oxford University Press, London, 1947), p. 175.